Optical and Thermal Behaviors of Plasmonic Bowtie Aperture and Its NSOM Characterization for Heat-Assisted Magnetic Recording

Xianfan Xu, Nan Zhou, Yan Li, and Luis Traverso

Birck Nanotechnology Center, School of Mechanical Engineering, Purdue University, West Lafayette, IN 47907 USA

Heat-assisted magnetic recording has the potential to keep increasing the areal density in the next-generation hard disk drives using a nanoscale optical antenna, called a near-field transducer (NFT), to locally and temporally heat a sub-diffraction-limited region in the recording medium. The NFTs made of plasmonic nanoscale optical antennas provide the capability of sub-wavelength light manipulation at optical frequencies. These antennas are designed using both plasmonic resonance and localized plasmons to produce an enhanced field in an area far below the diffraction limit. To reduce the self-heating effect in the NFT, which could cause materials failure that leads to the degradation of the overall hard drive performance, the NFT must deliver sufficient power to the recording medium with as small as possible incident laser power. In this paper, using the bowtie aperture as an example, we present the effect of optical properties on field localization, absorption, and coupling efficiency. Computations of heat dissipation and the induced temperature rise in the NFT are carried out to study their dependence on materials' properties. With the recent significant interests in alternative low-loss plasmonic materials in the visible and near-infrared range, the possibility of using alternative plasmonic materials for delivering higher power and simultaneously reducing heating in the NFT is investigated. The NFT characterization using scanning near-field scanning optical microscopy is also discussed.

Index Terms— **Heat-assisted magnetic recording (HAMR), near-field transducers (NFT), plasmonic materials, scattering-type scanning near-field optical microscopy (s-NSOM).**

I. Introduction

THE continuous growth in data storage is met by the increase in the areal data storage density. Heat-assisted magnetic recording (HAMR) [1]–[3] is being developed to keep increasing the areal density beyond 1.5 Pb/m^2 ($\sim$1 Tb/in^2) for the next-generation hard disk drives (HDDs). The key component for HAMR is a near-field transducer (NFT). The NFT helps reduce the magnetic coercivity by heating a small region in the recording medium locally and temporally. The NFTs are fundamentally plasmonic nanoscale optical antennas that are able to manipulate light in the sub-wavelength scale by producing an enhanced field spot less than 50 nm [4], which is used as a heating source in HAMR.

Plasmonic materials are typically metals. As a result, the temperature rise in the plasmonic NFT could be several hundred degrees because of heating. To avoid material and component failure during the heating process, the NFT must be designed to deliver enough power to the recording medium with as small as possible incident laser power to reduce the possible self-heating. Alternatively, there are efforts to develop alternative low-loss plasmonic materials in the visible and near-infrared range [5]. These alternative plasmonic materials can hold the potential in improving the thermal stability of an NFT. Fabricating NFTs using alternative plasmonic materials, for example, gold and silver alloys [6], [7], and nitride materials [8] has been reported.

There is also a demand for developing high resolution near-field microscopy systems to characterize the performance of an NFT. Scattering-type scanning near-field optical microscopy (s-SNOM or s-NSOM) can achieve a resolution on the order of 10 nm. Both amplitude and phase information can be obtained simultaneously using proper techniques [9]. A sharp atomic force microscope (AFM) tip oscillates and scans in the vicinity of the NFT. This sharp tip serves as a scatter, converting evanescent near-fields generated by the NFT to propagating radiation. The collected far-field signals are demodulated at higher harmonics of the tapping frequency, in order to suppress the background noise coming from the tip shaft and sample surface [10].

This paper reviews the effects of optical properties on field localization, absorption, and coupling efficiency of a plasmonic bowtie antenna, as well as the dependence of heat dissipation and temperature change on materials' properties. The possibility of using alternative plasmonic materials for delivering higher power and simultaneously reducing heating in the NFT is also discussed by the parametric studies. Results of NFT characterization using s-NSOM are also presented.

II. Effect of Optical Properties on Field Localization, Absorption, Coupling, and Thermal Efficiencies

A. Figure of Merit

The NFTs manipulate light primarily through the surface plasmons and/or localized surface plasmon resonance. The confined optical spot size determines the size of the thermal spot in the magnetic recording medium to reduce the bit size. The NFT needs to be designed to deliver optical power to the recording medium with the minimum heating of NFT itself. To prevent thermal damage to an NFT, it is important to evaluate its temperature evolution under laser irradiation. That is, the temperature of the media should be raised to above the Curie temperature while maintaining the temperature rise in the NFT as low as possible. Here, we use a thermal efficiency figure of merit, which is taken as the ratio of peak temperature rise in the recording medium to the peak temperature rise in

Manuscript received July 17, 2015; revised August 31, 2015 and September 14, 2015; accepted September 14, 2015. Date of publication September 17, 2015; date of current version January 18, 2016. Corresponding author: X. Xu (e-mail: xxu@ecn.purdue.edu).

Color versions of one or more of the figures in this paper are available online at http://ieeexplore.ieee.org.

Digital Object Identifier 10.1109/TMAG.2015.2479584

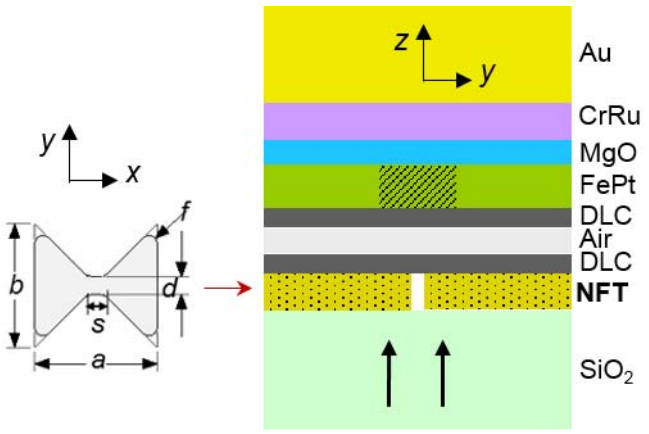

Fig. 1. Bowtie-shaped aperture NFT defined in a metallic film (not shown) and the simulated material stack.

the NFT

$$\text{Thermal efficiency} = \frac{\Delta T_{\text{peak, media}}}{\Delta T_{\text{peak, NFT}}}. \quad (1)$$

The performance of NFT and its thermal efficiency are determined by its optical and thermal properties. For a lossy material, the dissipated power density q scales linearly with the imaginary part of relative permittivity $\text{Im}(\varepsilon)$ and the field intensity $|E|^2$, expressed as

$$q = \frac{1}{2}\varepsilon_0 \omega \text{Im}(\varepsilon)|E|^2. \quad (2)$$

Reducing $\text{Im}(\varepsilon)$ and $|E|^2$ are two opportunities to minimize the heating effect in an NFT. The field intensity $|E|^2$ is largely determined by $\text{Re}(\varepsilon)$. A more negative $\text{Re}(\varepsilon)$ typically indicates a stronger plasmonic resonance, a larger field enhancement, and a better lateral energy confinement, which are favorable for the NFTs. Therefore, there is a field localization/enhancement penalty if minimizing the heat dissipation in the NFT by reducing $|E|^2/|\text{Re}(\varepsilon)|$. The effect of optical properties on field localization, dissipation in NFT, and the optical coupling and thermal efficiencies should all be considered to optimize the optical performance and improve the thermal efficiency.

B. Optical and Thermal Modeling of Bowtie Apertures in Gold and Silver Films

Recent reports have shown the candidates for HAMR NFTs, which are primarily plasmonic antenna-based, for example, the lollipop-shaped NFT [2], the E-shaped antenna [3], and the nanobeak-shaped antenna [11]. However, here, we use a bowtie aperture as the NFT design because of its good optical performance and it is a particularly tractable geometry for analysis, sample fabrication, and measurement. The bowtie aperture has attracted considerable attention as it supports not only the plasmonic effects but also the lightning-rod effect. It has also been shown that the propagating waveguide mode in a bowtie aperture enhances the optical transmission. An optical spot size smaller than 50 nm and with an acceptable coupling efficiency has been demonstrated using a plasmonic bowtie antenna [12].

We first perform a study to compare gold and silver bowtie apertures to illustrate the importance of low optical loss for the NFT applications. The optical and thermal properties of the materials are found in [13]. Fig. 1 shows the geometry of a bowtie NFT and the simulated material stack for the storage medium. Descriptions of the numerical model, including materials' properties at 800 nm wavelength, and the numerical details can be found in [13]. We evaluate the fraction of the laser power generated in the shaded 80 nm-diameter cylinder in the recording layer (FePt, 8 nm thick) due to laser heating. The dimensions of the aperture are fixed at $a = 400$ nm, $t = 90$ nm, and $s = d = 20$ nm, which have been optimized to provide the best coupling efficiency using gold as the NFT material [13]. It is noted that the NFT feature size will be different when the material changes. Therefore, the results we presented in this session are illustrative for the trend.

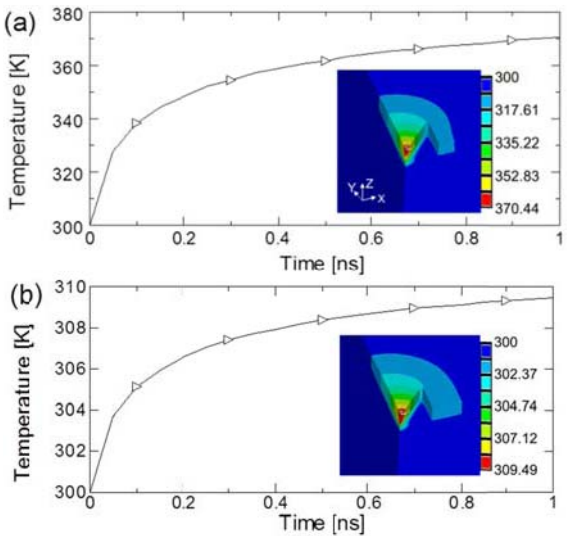

Fig. 2. Temperature distributions in the NFT for (a) gold and (b) silver bowtie apertures. The corresponding spatial distributions are calculated at 1 ns.

From our calculation, it is found that the coupling efficiency for a silver bowtie aperture is 4.37%, slightly better than 4.04% with the same aperture made in gold. The major difference between silver and gold is that the silver has a much smaller imaginary part of the permittivity ($\varepsilon_{\text{Ag}} = -30.98 + 0.4i$). Therefore, the absorption rate in the whole silver film is 1.28%, much smaller than the 6.97% in gold ($\varepsilon_{\text{Au}} = -24.06 + 1.52i$).

The calculated optical power is the heat source for computing the temperature rise in both the NFT and the media stack. In the calculation, a total laser power of 40 mW is focused to a spot size of 0.3 μm. This power was used to raise the temperature in the recording medium above its Curie temperature, ~750 K.

The temperature distribution for the peak temperature node is shown in Fig. 2(a) and (b) for the bowtie apertures made in gold and silver films, respectively. The temperature increases quickly at first and then is approaching the steady state ~1 ns. Note that 1 ns is about the time a bit is heated. While the NFT is heated for longer than 1 ns, the calculation results indicate its temperature tends to saturate after 1 ns. At 1 ns, the spatial temperature distribution shows that the peak temperature occurs at the tip of the bowtie aperture facing the laser irradiation. This is intuitive because the field enhancement is most intense at the tip of the bowtie. Because of the low absorption in silver, the temperature rise is much smaller for the bowtie aperture made in a silver film. On the other hand, the corresponding temperature rises in the recording media are comparable, as shown in Fig. 3.

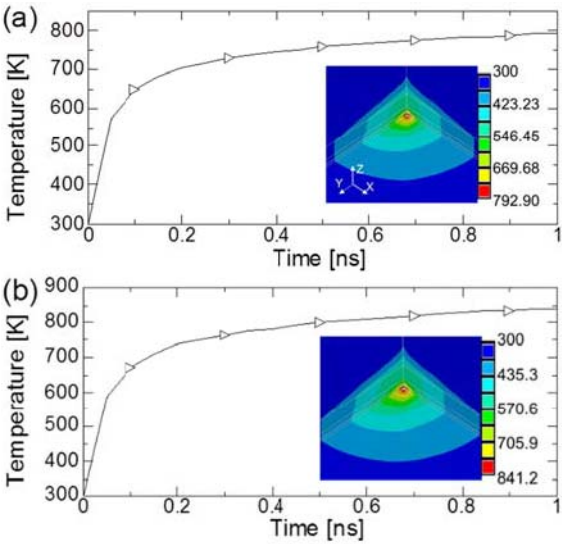

Fig. 3. Temperature distributions in the recording stack for (a) gold and (b) silver bowtie apertures. The spatial distributions are calculated at 1 ns.

TABLE I
COMPARISON BETWEEN GOLD AND SILVER NFTs

Quantity	Au	Ag	FOM(Au/Ag)
Re(ε)	-24.06	-30.98	0.78
Im(ε)	1.52	0.4	3.8
Coupling efficiency	4.04%	4.37%	0.92
Absorption in NFT film	6.97%	1.28%	5.45
ΔT in NFT	70.4 K	9.5 K	7.41
ΔT in media	492.9 K	541.2 K	0.91
Thermal efficiency	7.0	57.0	1/8.14
Thermal diffusivity (RT)	127×10^{-6} m^2/s	174×10^{-6} m^2/s	0.73

From the calculation results, we can obtain the thermal efficiency defined in (1). A detailed comparison is summarized in Table I, where the last column is the ratio between gold and silver bowtie apertures for each quantity. A silver NFT provides a slightly better coupling efficiency, which leads to a slightly higher peak rise $\Delta T = 541.2$ K in the recording media. The small absorption in the silver film directly leads to a small $\Delta T = 9.5$ K in the silver NFT, while $\Delta T = 70.4$ K in the gold NFT. Note that the ratio of ΔT in the NFT is 7.41, which is higher than 5.45, the ratio of absorption in the NFTs. This could be attributed to the different thermal transport properties, which leads to $5.45/0.73 \approx 7.47$. The thermal efficiency of the silver bowtie aperture is computed to be 57, which is ~8 times that of gold (~7).

C. Effect of Optical Properties

In order to improve the reliability of NFT, it is important to search for low-loss materials in the near-infrared wavelength range. The success may pave the way for simultaneously delivering the sufficient optical power to the medium and minimizing heating in the NFT.

A parametric study was conducted for the optical properties of NFT materials and the results are shown in Figs. 4 and 5. The dependence of the optical coupling efficiency and the optical absorption in the NFT on the imaginary part of the dielectric constant Im(ε) and real part Re(ε) is shown in Fig. 5.

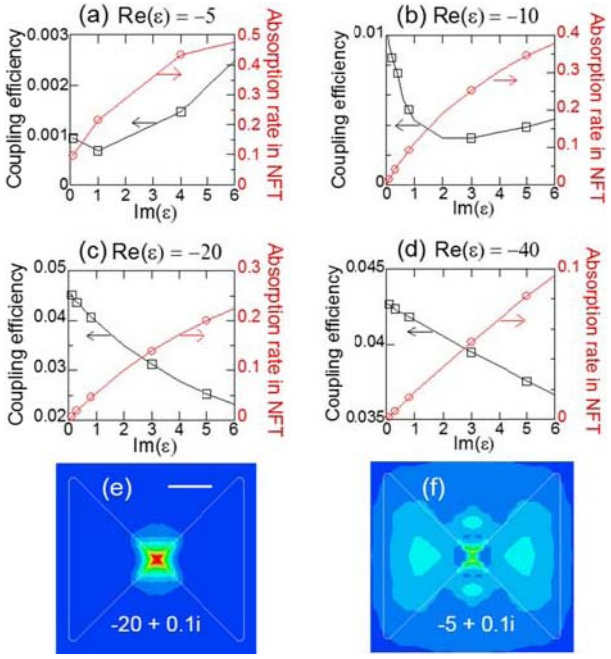

Fig. 4. (a)–(d) Coupling efficiency and absorption rate in the NFT as a function of Im(ε) at four Re(ε) values. Absorption distributions in FePt with (e) Re(ε) = −20 and Im(ε) = 0.1, and (f) Re(ε) = −5 and Im(ε) = 0.1. The scale bar in (e) is 100 nm and is applicable to (f).

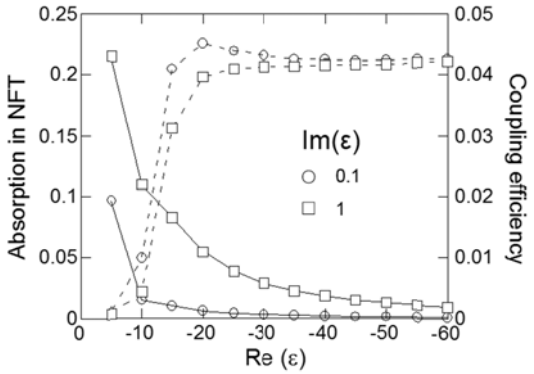

Fig. 5. Dashed lines: effect of permittivity on coupling efficiency and absorption rate in the NFT, as a function of Re(ε) at two Im(ε) values 0.1 and 1.

It is seen that the absorption increases almost linearly with the increase of Im(ε). This is consistent as what is shown in (1). The coupling efficiency should decrease with Im(ε), however, this is only seen when |Re(ε)| is large ($\geq$20). When |Re(ε)| is small, the field produced by the NFT cannot be localized, and the field is only localized when |Re(ε)| is large enough. It is seen that for Re(ε) = −20 and Im(ε) = 0.1, a strong field confinement in the central plane of the FePt layer is shown in Fig. 4(e) with an FWHM size of $37(x)\times39(y)$ nm^2. The best optical coupling efficiency is calculated to be 4.5%. The corresponding absorption rate in the NFT is only 0.61%. On the other hand, it is calculated with Re(ε) = −5 and Im(ε) = 0.1, the material is not metallic and plasmonic enough so the absorbed light is not localized as shown in Fig. 4(f).

Fig. 5 interprets the parametric study in a different way by plotting the result as a function of Re(ε) at two different values of Im(ε). The results again indicate that it is impropriate to use small |Re(ε)|, consistent with (1). When the loss is negligible, Im(ε) = 0.1, there exists an optimized Re(ε) to achieve the

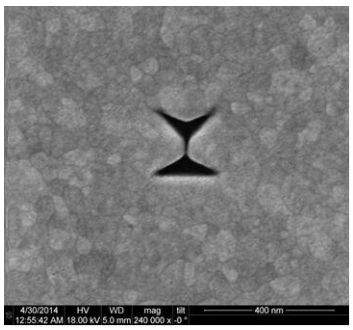

Fig. 6. SEM image of the fabricated bowtie aperture.

maximum coupling efficiency as shown. For a relatively larger loss term, $\mathrm{Im}(\varepsilon) = 1$, a relatively large $|\mathrm{Re}(\varepsilon)|$ is preferred to produce a better coupling efficiency and smaller dissipation in an NFT at the same time.

III. Scattering-NSOM for Characterizing NFTs

To characterize NFTs, a s-NSOM system was developed, which is custom-built based on a commercial AFM platform (CombiScope 1000, AIST-NT Inc.). The resolution of the measurements is determined by the size of the curvature of the tip apex, which is much smaller than the diffraction limit. An accurate interpretation of the field produced by an NFT requires characterizing both the in-plane and out-of-plane components of the fields. Therefore, we developed a method for detecting different field components. The field distribution in the space above the NFT was also measured. With these considerations, the mapping of NFT produced near fields was extended to 3-D space. This provides a complete characterization of the complex vector fields around the designed NFT structures.

A. Experimental Details

Fig. 6 shows the SEM image of the bowtie aperture. It was made in a 60 nm thick gold film coated on a glass substrate. The designed dimension has an outline of 150 nm with a designed gap size ~20 nm. It is noticed that the sample always has tapered side walls and enlarged aperture size caused by the milling using the focused ion beam (FEI Nova 200 dual-beam FIB). The undesired taper of the side walls will lead to both the field localization and enhancement penalties [14].

The scanning process for the 3-D mapping is discussed in detail in [15] and briefly described as follows.

The homemade s-SNOM can work under both reflection and transmission modes. For NFT characterization, the transmission mode is applied and a 633 nm HeNe laser illuminates the sample from the substrate.

B. 3-D Characterization of the Bowtie Aperture NFT

Fig. 7 shows the amplitude and phase distributions of the E_z field. The optical field distribution is overlapped with the AFM measured topography (back shading) that was obtained simultaneously with the s-NSOM data, illustrating the exact relation between the sample structure and the measured near-field. Fig. 7(b) shows the localization of the E_z field near the edges of the bowtie aperture gap. The fields are tightly bounded to the bowtie metal surface and are following the curvatures of the edges. The curvatures in the fabricated

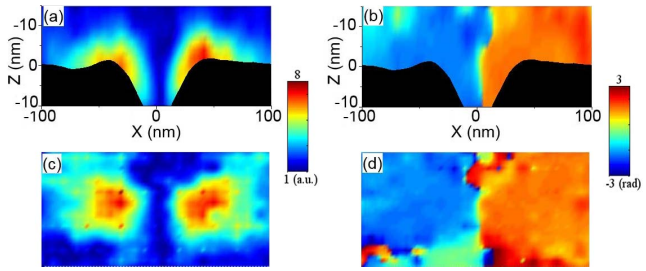

Fig. 7. Mapped (a) amplitude and (b) phase in xz plane across the bowtie aperture. Mapped (c) amplitude and (d) phase images in xy plane at $z = 0$. The sizes of (c) and (d) are 200 nm × 100 nm.

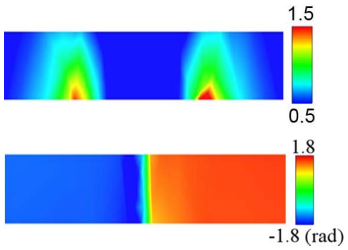

Fig. 8. Simulated amplitude and phase of E_z in the xz plane. Image sizes are 200 nm × 15 nm.

antenna lead to spread hot spots over the corner, degrading the field confinement. The characteristic 180 degrees phase shift between the spots is also clearly resolved in Fig. 7(b). The calculated amplitude and phase distributions in the xz plane are shown in Fig. 8. It generally confirms the validity of the experiment results. The dimensions of the model used in the simulation are from the AFM topography measurement [15]. From Fig. 7, we are able to see field variation within a vertical distance of ~1 nm. This demonstrates that because of the strong dipole–dipole-like interaction between the tip and the sample, the s-SNOM is capable of providing a resolution of a few nanometers in the z-direction.

IV. Conclusion

By performing optical and thermal simulations of the bowtie aperture NFTs with the presence of a recording media stack, we discuss the effects of optical properties on field localization, absorption, coupling, and thermal efficiencies. The study comparing gold and silver bowtie apertures demonstrates that, with a much smaller loss, silver provides a thermal efficiency 8 times that of gold. Parametric studies of optical properties indicate that it is possible to deliver higher power and reduce heating simultaneously in the NFT using materials with as small as possible loss and a moderately large real part of the permittivity. We also apply s-NSOM to obtain the 3-D amplitude and phase of the optical near-fields produced by a bowtie aperture NFT, with a high lateral resolution of tens of nanometers and a vertical resolution better than a few nanometers. Such characterizations will be useful for the development of NFTs for HAMR.

Acknowledgment

This work was supported in part by the Defense Advanced Research Projects Agency under Grant N66001-08-1-2037, in part by the National Science Foundation under

Grant CMMI-1120577, and in part by the Advanced Storage Technology Consortium. The authors would like to thank W. Nam for assistance with the sample fabrication.

REFERENCES

[1] M. H. Kryder *et al.*, "Heat assisted magnetic recording," *Proc. IEEE*, vol. 96, no. 11, pp. 1810–1835, Nov. 2008.

[2] W. A. Challener *et al.*, "Heat-assisted magnetic recording by a near-field transducer with efficient optical energy transfer," *Nature Photon.*, vol. 3, pp. 220–224, Mar. 2009.

[3] B. C. Stipe *et al.*, "Magnetic recording at 1.5 Pb m^{-2} using an integrated plasmonic antenna," *Nature Photon.*, vol. 4, pp. 484–488, May 2010.

[4] W. A. Challener, E. Gage, A. Itagi, and C. Peng, "Optical transducers for near field recording," *Jpn. J. Appl. Phys.*, vol. 45, no. 8S, pp. 6632–6642, 2006.

[5] G. V. Naik, V. M. Shalaev, and A. Boltasseva, "Alternative plasmonic materials: Beyond gold and silver," *Adv. Mater.*, vol. 25, no. 24, pp. 3264–3294, Jun. 2013.

[6] M. Zhu, T. Zhao, S. C. Riemer, and M. C. Kautzky, "HAMR NFT materials with improved thermal stability," U.S. Patent 0 286 799 A1, Oct. 31, 2013.

[7] T. Zhao, M. C. Kautzky, W. A. Challener, and M. A. Seigler, "HAMR NFT materials with improved thermal stability," U.S. Patent 8 427 925 B2, Apr. 23, 2013.

[8] T. Zhao, S. Sahoo, M. C. Kautzky, and A. V. Itagi, "Near field transducers including nitride materials," U.S. Patent 0 279 315 A1, Oct. 24, 2013.

[9] F. Keilmann and R. Hillenbrand, "Near-field microscopy by elastic light scattering from a tip," *Philos. Trans. Roy. Soc. London A, Math. Phys. Sci.*, vol. 362, no. 1817, pp. 787–805, 2004.

[10] Y. Li, N. Zhou, E. C. Kinzel, X. Ren, and X. Xu, "The origin of interferometric effect involving surface plasmon polariton in scattering near-field scanning optical microscopy," *Opt. Exp.*, vol. 22, no. 3, pp. 2965–2972, 2014.

[11] T. Matsumoto, F. Akagi, M. Mochizuki, H. Miyamoto, and B. Stipe, "Integrated head design using a nanobeak antenna for thermally assisted magnetic recording," *Opt. Exp.*, vol. 20, no. 17, pp. 18946–18954, 2012.

[12] N. Zhou, E. C. Kinzel, and X. Xu, "Nanoscale ridge aperture as near-field transducer for heat-assisted magnetic recording," *Appl. Opt.*, vol. 50, no. 31, pp. G42–G46, 2011.

[13] N. Zhou, L. M. Traverso, and X. Xu, "Power delivery and self-heating in nanoscale near field transducer for heat-assisted magnetic recording," *Nanotechnology*, vol. 26, no. 13, p. 134001, 2015.

[14] N. Zhou, Y. Li, and X. Xu, "Resolving near-field from high order signals of scattering near-field scanning optical microscopy," *Opt. Exp.*, vol. 22, no. 15, pp. 18715–18723, 2014.

[15] Y. Li, N. Zhou, and X. Xu, "Three-dimensional mapping of optical near field with scattering SNOM," *Opt. Exp.*, vol. 23, no. 14, pp. 18730–18735, 2015.